The Owen Ridge uplift in the Arabian Sea: Implications for the sedimentary record of Indian monsoon in Late Miocene

Mathieu Rodriguez, Nicolas Chamot-Rooke, Philippe Huchon, Marc Fournier, Matthias Delescluse

PREPRINT *Earth and Planetary Science Letters* 394 (2014) 1–12

The Owen Ridge uplift in the Arabian Sea: implications for the sedimentary record of Indian monsoon in Late Miocene

Mathieu Rodriguez[1*], Nicolas Chamot-Rooke[1], Philippe Huchon[2,3], Marc Fournier[2,3], Matthias Delescluse[1]

(1) Laboratoire de Géologie de l'Ecole normale supérieure de Paris; CNRS UMR 8538, 24 rue Lhomond, 75005 Paris, France

(2) Institut des Sciences de la Terre de Paris, CNRS UMR 7193, Université Pierre & Marie Curie, case 129, 4 place Jussieu, 75005 Paris, France

(3) iSTeP, UMR 7193, CNRS, F-75005 Paris, France

**Corresponding author*: rodriguez@geologie.ens.fr

Abstract

The pelagic cover of the Owen Ridge in the Arabian Sea recorded the evolution of the Indian monsoon since the Middle Miocene. The uplift of the Owen Ridge resulted from tectonic processes along the previously unidentified Miocene India-Arabia plate boundary. Based on seismic reflection data tied with deep-sea drilling to track the Miocene India-Arabia plate boundary, we propose a new timing for the uplift of the Owen Ridge and highlight its impact on the record of climate changes in pelagic sediments. The new dataset reveals a fracture zone east of the Owen Ridge corresponding to the fossil plate boundary, and documents that the main uplift of the Owen Ridge occurred close to ~8.5 Ma, and is coeval with a major uplift of the east Oman margin. Late Miocene deformation at the India-Arabia plate boundary is also coeval with the onset of intra-plate deformation in the Central Indian Ocean, suggesting a kinematic change of India and surrounding plates in the Late Miocene. The uplift of the Owen Ridge above the

lysocline at ~8.5 Ma accounts for a better preservation of *Globigerina bulloides* in the pelagic cover, previously misinterpreted as the result of a monsoon intensification event.

1. Introduction

The pelagic sedimentary cover of the Owen Ridge contains the past records of the Asian summer monsoon since the Middle Miocene (Shipboard Scientific Party, 1974, 1989). The ridge itself consists of a series of bathymetric highs sub-dividing the Arabian Sea into an abyssal plain to the east and a shallower Owen basin to the west (Fig. 1). The Arabian Sea is located on the migration path of the Inter Tropical Convergence Zone, which controls the seasonality of the Asian monsoon. The apparent increase in the abundance of the foraminifera *Globigerina bulloides* within the Owen Ridge's pelagic cover, commonly interpreted as a proxy for monsoon-driven upwelling (Kroon et al., 1991), suggests that the evolution of astronomical parameters alone cannot be responsible for the observed monsoon intensification in the upper Miocene (Molnar et al., 1993; Molnar, 2005; Sun and Wang, 2005; Huang et al., 2007; Clift et al., 2008; Steinke et al., 2010). A Late Miocene uplift of the Himalayan-Tibetan Plateau (Harrison et al., 1992) was proposed as a forcing mechanism over the climatic system, high elevation inducing a reorganisation of the atmospheric circulation and hence, monsoon intensification (Molnar and England, 1990; Molnar et al., 1993; Ann et al., 2001). However, a growing set of observations showed that the Himalaya mountain belt reached its present-day elevation at least ~15 Myrs ago, and probably earlier (Spicer et al., 2003; Molnar, 2005; Harris, 2006; Rowley and Currie, 2006; Dupont-Nivet et al., 2008; Wang et al., 2012; Yuan et al., 2013).

A re-analysis of marine sediments drilled at the Owen Ridge questioned the record of an apparent monsoon intensification at ~8.5 Ma (Huang et al., 2007). Selecting foraminifera of large size to remove the effect of variations in carbonate dissolution in the abundance records, Huang et al. (2007) document only a minor change in the fraction of *G. bulloides* near 10 Ma. The latter is consistent with a constant decrease in weathering of India during the Late Miocene (Clift et al., 2001; 2003; 2008). Steinke et al. (2010) even suggested that the Late Miocene was a period of summer monsoon weakening over India, rather than intensification.

55 The timing of seafloor uplift in the Indian Ocean is critical to the understanding of the sedimentary
56 record of climate during the Cenozoic. The commonly accepted tectonic framework of the Arabian
57 Sea is that the uplift of the Owen Ridge was coeval with the beginning of accretion at the Sheba Ridge
58 in the Gulf of Aden 20 Ma ago (Fig. 1) (Whitmarsh, 1979) and with the shift of the India-Arabia plate-
59 boundary from the Oman continental margin to its present-day location (Mountain and Prell, 1990).
60 However, structural and kinematic studies show that the Owen Fracture Zone (the current plate
61 boundary) is no older than 3 to 6 Ma (Fournier et al., 2008a; 2011; Rodriguez et al., 2011; 2013b). As
62 a result, the location of the India-Arabia plate boundary during the Miocene, as well as its relationship
63 with the uplift of the Owen Ridge, remain unknown.
64 Here we present a new set of seismic reflection data that documents a Late Miocene tectonic uplift at
65 the edges of the Owen Basin, including the Owen Ridge. We identify the Miocene India-Arabia plate
66 boundary and highlight the tectonic processes at the origin of the Owen Ridge uplift. We finally
67 discuss how the latter impacted the record of climate evolution in the pelagic sediments of the Arabian
68 Sea.
69

70 **2. Materials and methods**

71 The dataset presented in this study was acquired onboard the French Navy oceanographic vessel
72 *Beautemps-Beaupré* during the OWEN and OWEN-2 surveys run in 2009 and 2012 respectively.
73 Multibeam bathymetry was collected using a Kongsberg-Simrad EM 120 echo-sounder (Fig. 1, 2).
74 Seismic reflection profiles were acquired at 10 knots using two GI air-guns (one 105/105 c.i. and one
75 45/45 c.i., fired every 10 seconds at 160 bars in harmonic mode, resulting in frequencies ranging from
76 15 to 120 Hz) and a 24-channel, 600 m-long streamer, implying a common mid-point spacing of 6.25
77 m. A sub-surface penetration of about 2s two-way travel time (TWT) was achieved throughout the
78 survey. The processing consisted of geometry setting, water-velocity normal move-out, stacking,
79 water-velocity F-K domain post-stack time migration, bandpass filtering and automatic gain control.
80 All profiles are displayed with a vertical exaggeration of 8 at the seafloor. The seismic dataset is tied
81 with Deep Sea Drilling Project (DSDP) and Ocean Drilling Project (ODP) drillings available in the
82 Arabian Sea (Shipboard Scientific Party, 1974; 1989) to provide the stratigraphic framework (Fig. 3,

inset). Reflectors picked on seismic profiles have been selected based on seismic discontinuities that reflect lithological changes, stratigraphic hiatuses or tectonic deformation.

3. Geological framework of the Arabian Sea and the Owen-Murray Ridge System

3.1. *Present-day morphology of the Arabian Sea*

The Owen Fracture Zone is an 800-km-long strike-slip fault system, which runs along the Owen Ridge (Fig. 1). The southern Owen Ridge is a 300 km-long, 50-km wide, and up to 2000 m-high relief that appears as a vast tilted slab (Fig. 2b). It contrasts with the uneven topography of the 220 km-long, 50 km-wide, and up to 1700 m-high central ridge (Fig. 2a), and the guyot morphology of the Qalhat Seamount further to the north. The Owen Fracture Zone connects seafloor spreading at the Sheba mid-oceanic ridge with the Makran subduction zone (Fig. 1). At its northern end, the Owen Fracture Zone forms a complex stepover basin known as the Dalrymple Trough (Edwards et al., 2000; Gaedicke et al., 2002), which is flanked to the east by the Murray Ridge. Seafloor spreading at the Sheba Ridge started around 20 Ma (Fournier et al., 2010), whereas subduction in the Makran area began in the Late Cretaceous (McCall, 1997). The modern accretionary wedge developed since the Tortonian (7.2-11.6 Ma) (McCall, 1997; Burg et al., 2008; Smit et al., 2010). Seafloor morphology does not display any trace of the Miocene India-Arabia plate boundary (Rodriguez et al., 2011).

3.2. *Substratum of the Owen-Murray Ridge System*

Several seismic lines run as pre-site surveys for DSDP and ODP reached the basement of the southern and the central ridges. Their uneven substratum, drilled at DSDP Sites 223 and 224 (Fig. 2), is basaltic in composition and of Late Paleocene age (Shipboard Scientific Party, 1974; 1989). These 50-55 Ma-old reliefs might either be tilted slivers of oceanic crust or volcanic highs (Fig. 3b), and are hereafter referred as the "pre-Owen Ridge". The history of the Murray Ridge basement is not clearly established, since it has never been drilled. Based upon seismic refraction data, the Murray Ridge has been interpreted as a small piece of continental crust inherited from the Gondwana break-up (Edwards et al., 2000; 2008).

3.3. *Uplift of the Owen Ridge*

In its present-day configuration, the southern Owen Ridge is formed at its top by Upper Oligocene-Lower Miocene turbidites coming from the Indus deep-sea fan and the subsequent pelagic cover (Fig. 3b) (Shipboard Scientific Party, 1974; 1989). Lower Miocene turbidites at the top of the Owen Ridge indicates an episode of uplift during the Miocene, rejuvenating the topography of the proto-Owen Ridge.

So far, the uplift of the Owen Ridge has been dated at 20 Ma based on two sets of arguments. The first set of arguments deals with the progressive burial of the proto-Owen Ridge and its pelagic cover by Upper Oligocene-Lower Miocene Indus turbidites, which forms a diachronous angular unconformity (picked in light purple) (Fig. 3) biostratigraphically dated at 19.6 Ma and ~14 Ma at the southern (Fig. 3b) and central (Fig. 3c) Owen Ridge, respectively (Shipboard Scientific Party, 1974). In fact, this angular unconformity is unrelated to any tectonic uplift of the Owen Ridge, in contrast with previous interpretation by Whitmarsh et al. (1974; 1979). Second, the transition from Indus turbidites to Miocene pelagic deposits drilled on the southern Owen Ridge at DSDP Site 224 and ODP Sites 721, 722, 731 (top of Unit 4, Fig. 3) has been considered by Mountain and Prell (1990) as an indicator of uplift above the level of turbiditic deposition. The transition is marked by a mixed pelagic-turbiditic sequence biostratigraphically dated at 14-15 Ma, composed of thin detrital particles, interpreted as the uppermost part of the turbiditic plume being deposited during the first stages of ridge uplift (Mountain and Prell, 1990). The latter argument will be revised in the light of our new dataset.

3.4. *Past locations of the India-Arabia plate-boundary*

Past location of the India-Arabia plate boundary prior to the Owen Fracture Zone is currently unknown. Early paleogeographic reconstructions by Whitmarsh (1979) suggested that the India-Arabia plate boundary was already at its present-day location when India started to move northwards at ~90 Ma. An alternative paleogeographic reconstruction (Mountain and Prell, 1990) postulates that the India-Arabia plate-boundary initially ran along the Oman continental margin, while the Mascarene Basin opened between Madagascar and Seychelles (between ~90-60 Ma) (Bernard and Munschy, 2000) and the Carlsberg Ridge developed (since ~63 Ma; Dyment, 1998). The India-Arabia plate-

boundary would then have jumped to its present-day position in the Early Miocene (~20 Ma), triggering the uplift of the Owen Ridge (Mountain and Prell, 1990). A Paleogene location of the India-Arabia plate-boundary in the Owen Basin is also supported by paleogeographic reconstructions based on the record of magnetic anomalies over the Arabian Sea (Royer et al., 2002).

4. Results

4.1. *Late Miocene deformation and contourites on the East-Oman margin*

Seismic profiles crossing the edge of the continental platform reveal a large, ~20-km-wide anticline affecting Lower to Upper Miocene sediments composed of calcareous turbidites according to the nearby ODP Site 730 (units U2 and U3, Fig. 3a and 4) (Shipboard Scientific Party, 1989). A dense network of faults affects the anticline and is sealed by upper Miocene to Plio-Pleistocene deposits (unit U1, Fig. 3a and 4). The folded unit contains planktonic faunas typical of a deep-sea environment (Shipboard Scientific Party, 1989). An erosive surface sealing the top of the anticline (Fig. 3a and 4) indicates local uplift of the platform during the folding episode. At the location of the ODP Site 730, the fold then subsided down below the sea level in early Pleistocene times, as indicated by the age of the first overlying sediments (1.3 Ma). Thick chaotic bodies interpreted as Mass Transport Deposits (MTD hereafter) on Fig. 3a and 4 are observed down the eastern flank of the fold, indicating sudden slope over-steepening related to the formation of the fold. The youngest calcareous turbidites affected by the deformation are ~8.8 Ma-old according to correlations with ODP Site 730. The fold is overlaid by ~8.2 Ma-old sediments according to ODP Site 728 (Shipboard Scientific Party, 1989). This set of observations documents a major uplift episode along the Oman margin around 8.5 Ma.

Bottom currents influenced the architecture of the sedimentary unit U1 sealing the fold (Fig. 3a). Unit 1 displays a complicated set of imbricated, sigmoid to undulating geometries, all non-parallel to the accumulation surface that moved preferentially upslope through times. This description corresponds to a confined drift according to the classification of Faugères et al. (1999), and is very similar to drifts observed along the Algarve Margin (Portugal) (Marchès et al., 2010; Brackenridge et al., 2013).

4. 2. *Late Miocene deformation at the Southern Owen Ridge*

An E-W seismic line was acquired close to ODP Site 722 on the Southern Owen Ridge, where the most complete sequence has been drilled (Fig. 3b). A fanning configuration characterizes the lower Miocene turbidites on top of the Owen Ridge (Fig. 3b, 5a, 5b, 6a). The seismic profile crossing ODP Site 722 (Fig. 3b) shows that the 14-15 Ma-old turbiditic-pelagic facies has been drilled on the levee of a fossil turbiditic channel. The ~40-m-deep channel axis is identified by a typical lens-like architecture and discontinuous, high-amplitude reflections. The associated levees display a characteristic wedge shape with high-amplitude, transparent seismic facies (Fig. 3b).

The sedimentary cover overlying the last turbiditic channel (units U3 to U1) is composed of pelagic deposits (Fig. 3, 5, 6). Pelagic Unit 3 displays slight lateral thicknesses variations (<0.1 s TWT), which results either from MTDs coming from the proto- Owen Ridge that still stood above the seafloor before the uplift, or from fanning related to a moderate tectonic activity (Fig. 5 a, b).

The transition between units 3 and 2 is marked by an increase of the sedimentation rates (from 15 to 54 $m.Ma^{-1}$) (Shipboard Scientific Party, 1989). Unit 2 is also marked by the appearance of submarine failures around ~8.5 Ma according to the nearby ODP Sites 721 and 731 (Fig. 2, 3, 5). The age of ~8.5 Ma corresponds to the age of the Foraminifera (*Discoaster hamatus*) immediately overlying the sedimentary hiatus (formed by the submarine failure) drilled at ODP Site 721. The configuration of submarine failures observed in the uppermost part of the pelagic sequence shows that the sediment failed and were transported in the direction of the Owen Basin (Fig. 3, 5), which indicates that the Owen Ridge was already uplifted at ~8.5 Ma. The thickness of Unit 2 increases in the southernmost part of the Owen Ridge, where it displays a conspicuous fanning pattern (Fig. 6a), starting at ~10 Ma, and ending at 8.5 Ma (first pelagic layer over the MTD that seals the fanning). The sedimentary sequence at the top of the Owen Ridge is faulted throughout its entire thickness (Fig. 3b and 5a) by a dense network of faults very similar to what is observed on the Oman margin (Fig. 3a). These faults display very irregular offsets and do not root into the basement (Fig. 6a). We interpret these faults as the result of fluid circulation (i.e. polygonal faults as defined in Cartwight, 1994). The change of sedimentary setting induced by the uplift of the southern ridge and the margin sealed fluid circulation in most places. At the southern ridge, fluid circulation may have controlled the distribution of submarines failures (Rodriguez et al., 2012).

195 Several folds are observed in the Indus abyssal plain at the eastern foot of the southern Owen Ridge,
196 and south of the Beautemps-Beaupré Basin (Fig. 5c, 6). A sharp and vertical fault plane, interpreted as
197 a fracture zone, crosscuts the eastern side of the Owen Ridge at depth (Fig. 6b, 6c; 7a). A system of
198 fossil folds buried under Indus deposits and MTDs coming from the ridge is observed east of the
199 southern ridge. The growth anticline displayed in Fig. 6c shows that compressive deformation is still
200 active at the Owen Fracture Zone (Rodriguez et al., 2011). The series of folds observed south of the
201 Beautemps-Beaupré Basin (Fig. 6d) display an isopach pattern at depth. The overlying deposits show
202 angular unconformities indicating several discontinuities in episodes of folding. Unfortunately, the
203 penetration of the nearby ODP Site 720 (location on Fig. 1) is too shallow to provide confident dating
204 of the initiation of this compressive episode. These folds could correspond either to the Owen Ridge
205 uplift at 8.5 Ma or to the emplacement of the Owen Fracture Zone between 3-6 Ma.
206
207 4.3. *Late Miocene deformation at the Central Owen Ridge and mass transport deposits*
208 Seismic profiles crossing the eastern side of the Central Owen Ridge document an angular
209 unconformity within the Indus deep-sea fan (blue in Fig. 7). The angular unconformity becomes
210 laterally concordant with the overlying sediments from the Indus fan. This key reflector is about 1 s
211 TWT deep in the undeformed area, which roughly corresponds to a Late Miocene age according to the
212 nearby DSDP Site 222. A sub-vertical fracture zone is identified at the eastern edge of the central
213 ridge (Fig. 7a).
214 DSDP Site 223 is located west of the central segment of the Owen Ridge, where the Early Miocene
215 unconformity was first determined (Shipboard Scientific Party, 1974; Whitmarsh, 1979). A second,
216 younger unconformity is observed both in the Owen Basin (Fig. 5d) and at the top of the central Owen
217 Ridge (Fig. 7), where it is underlined by MTDs composed of upper Miocene sediments (Fig. 3c)
218 overlying diatoms-rich sediments dated at 10 Ma (Shipboard Scientific Party, 1974). The reflector
219 corresponding to the top of the MTDs is correlated with sediments at the top of the Central Owen
220 Ridge. The overlying pelagic layer is 0.3 s (TWT) thick at the top of the central ridge, and devoid of
221 MTDs. The thickness of 0.3 s (TWT) is the same as Unit 1 on the Southern Owen Ridge in areas
222 undisturbed by submarine failures (Fig. 3). Assuming a pelagic sedimentation rate similar to the one

223 estimated at the southern ridge (Bourget et al., 2013) implies a Late Miocene age of the unconformity
224 (~8 Ma), consistent with the MTDs drilled downslope at DSDP Site 223. A similar unconformity
225 sealed by 0.3s (TWT) of pelagic sediments is observed at the top of most of the bathymetric highs
226 buried by the Indus fan and sediments from the Oman margin in the Owen Basin (Fig. 5 c). These
227 observations suggest a regional tectonic deformation at the origin of the ~8 Ma-old unconformity and
228 the uplift of the central Owen Ridge.
229
230 **5. Discussion**
231 5. 1. *Age of uplift of the Owen Ridge and Late Miocene deformation in the Owen Basin*
232 The Late Miocene episode of deformation (~8-9 Ma) described above contrasts with the 15-20 Ma age
233 previously assessed for the major uplift of the Owen Ridge (Whitmarsh, 1979; Mountain and Prell,
234 1990). The main argument in favour of a 15-20 Ma-old uplift of the Owen Ridge was the 14-15 Ma-
235 old mixed turbiditic-pelagic facies drilled at ODP Sites (Mountain and Prell, 1990). Because of its
236 location on a turbiditic levee (Fig. 3), the mixed facies cannot be interpreted by itself as the first stage
237 of the southern ridge uplift. During their deposition along turbiditic channels, turbiditic plumes
238 frequently undergo flow-stripping or overspilling processes (Piper and Normark, 1983; Hiscott et al.,
239 1997). These processes imply that the uppermost part of the turbiditic plume, composed of the thinner
240 detritic particles, overflows throughout the channel axis, leading to the deposition of mixed turbiditic-
241 pelagic sequence on turbiditic levees similar to the one described at ODP Site 722. The overlying
242 pelagic deposits (Units 2-3) simply reflect a shift in the locus of turbidites deposition. Thick pelagic
243 layers (>100 m-thick) are common features of the Indus deep-sea fan (DSDP Site 222, Shipboard
244 Scientific Party, 1974; ODP Site 720, Shipboard Scientific Party, 1989), where the alternation of
245 turbidites within pelagic sequences is controlled by avulsion processes, and not by seafloor uplift.
246 The lysocline is currently at a depth of ~4000 m in the area (Kolla et al., 1976) and its Miocene depth
247 is unknown, making it difficult to discriminate whether fluctuations in the conditions of microfossils
248 preservation throughout Unit 3 reflect the first stage of uplift of the Owen Ridge or oscillations in the
249 lysocline depth. Slight lateral thickness variations (~ 0.1 s (TWT)) of Unit 3 (10.4 to 14-15 Ma) may

250 indicate nearby tectonic activity (Fig. 3; 5a,b), but with no major topographic building during the
251 deposition of Unit 3.
252 The ~8.5-9 Ma onset of major submarine failures is a striking feature of both the southern and the
253 central Owen Ridges (Rodriguez et al., 2012; 2013a). The large expansion of the failure-related
254 erosive surface over both ridge segments, together with the erosive surface observed at the top of
255 buried reliefs in the Owen Basin and the synchronicity with the formation of anticlines along the
256 Oman margin strongly suggest that they all relate to a common regional tectonic event.
257 The 8-9 Ma age of deformation in the Owen Basin fits with the estimated Tortonian age (7.2-11.6 Ma)
258 of the post-rift uplift episode observed along the Dhofar margin in the Gulf of Aden (Platel and Roger,
259 1989; Lepvrier et al., 2002; Fournier et al., 2004; Petit et al., 2007; Gunnel et al., 2007; Bache et al.,
260 2010). Several local processes have been invoked for the uplift episode in the Dhofar (Bache et al.,
261 2010; Leroy et al., 2010), but the Late Miocene episode of deformation identified in the Owen Basin
262 could better account for this uplift as rifted areas are prone to be reactivated by intra-plate deformation
263 (e.g. Cloetingh et al., 2008). On the other hand, the reassessed age of deformation in the Owen Basin
264 contrasts with the age of uplift of the Murray Ridge estimated at ~20 Ma (Clift et al., 2001; Gaedicke
265 et al., 2002). This discrepancy may reflect either the lack of good stratigraphic control of the
266 deformation in the vicinity of the Murray Ridge, or a different tectonic episode. Recent ties with
267 industrial drillings (Calvès, 2008) shows that the youngest turbidites tilted by the uplift of the Murray
268 Ridge are actually 8-10 Myr-old.
269
270 5. 2. *Uplift of the Owen Ridge and the Early-Middle Miocene India-Arabia boundary*
271 The fracture zone segments observed at the eastern edge of the Owen Ridge (Fig. 6b, 6c) likely
272 correspond to the fossil India-Arabia plate-boundary in Early-Middle Miocene times, prior to the onset
273 of the Owen Fracture Zone. The system of buried fold observed on Fig. 5c probably marks the
274 deformation related to the Owen Ridge uplift. The fossil plate boundary must have been very weak to
275 allow the >2000 m uplift of the Owen Ridge. Based on free-air gravimetry and seismic profiles
276 analysis, Weissel et al. (1992) showed that the uplift of the Owen Ridge may have occurred as a
277 flexural response to either an extensional or a compressive event, making the tectonic interpretation of

278 the ridge ambiguous. Vertical deformation within the oceanic lithosphere is mainly controlled by the
279 lithospheric strength, which is a direct function of the thermal state - and therefore the age - of the
280 lithosphere (Weissel et al., 1992). Consequently, even a slight change in the stress field can generate
281 prominent seafloor uplift (>1000 m) of flexural origin in areas of strong rheological contrasts (i.e. the
282 India-Arabia plate-boundary and the Oman margin).
283 The uplift of the Owen Ridge may be responsible for the transition from the Miocene plate boundary
284 to the Owen Fracture Zone. The vertical offset along the fracture zone might have changed the stress
285 field around it, leading to the formation of a nearby new transform segment while the initial one
286 became extinct, in a way similar to what inferred for normal faults dynamics (Buck et al., 1993;
287 Bonatti et al., 2005). In this framework, the 3-6 Ma-old Owen Fracture Zone (Fournier et al., 2008a,
288 2008b; 2011) is a new transform segment located only 5-10 km from the previous segment (Fig. 6).
289 Considering that the uplift started around 10.5 Ma, the early-middle Miocene boundary accommodated
290 vertical motion during several million years prior to the onset of the Owen Fracture Zone. This
291 structural reorganization of the India-Arabia plate-boundary did not involve any significant change in
292 the direction of the India-Arabia relative motion, according to the kinematics reconstructions of
293 Chamot-Rooke et al. (2009).
294
295 5. 3. *Origin of the Late Miocene deformation in the Owen Basin*
296 The 15-20 Ma uplift of the Owen Ridge used to be related with the onset of seafloor spreading at the
297 Sheba Ridge (Cochran, 1981; Mountain and Prell, 1990). The Late Miocene age of uplift of the Owen
298 Ridge requires another tectonic trigger.
299 In the Arabian Sea, the magnetic anomalies observed over the Carlsberg (Somalia-India motion) and
300 the Sheba ridges (Somalia-Arabia motion) documents a slow deceleration of seafloor spreading rates
301 between 20 and 10 Ma, then followed by nearly constant spreading rates after 8-10 Ma (DeMets et al.,
302 2005; Merkouriev and DeMets, 2006; Fournier at al., 2010). A two-phases growth of compressive
303 folds is recognized in the Central Indian Ocean, the first and minor one being dated at ~14-15 Ma
304 (Krishna et al., 2009), and the second, major one, at 8-9 Ma (Weissel et al., 1980; Wiens et al., 1985;
305 Cochran et al., 1989; Bull and Scrutton, 1990, 1992; Chamot-Rooke et al., 1993; Delescluse et al.,

306 2008a; Bull et al., 2010). Age of the intraplate extension, counterpart of the intraplate compression, is
307 also compatible with a beginning of widespread deformation within the Indo-Australian plate around
308 10 Ma (Henstock et al., 2004). It suggests that the entire plate was subjected to a kinematic change
309 around 8-10 Ma, affecting both the plate interior and its boundaries.
310 The origin of the kinematic change responsible for the Indo-Australian intraplate deformation is a
311 matter of debate. Clark (2012) proposed a convergence of India with respect to Eurasia smoothly
312 decreasing through time since the very beginning of the collision, as a result of the viscous resistance
313 exerted by the lithospheric mantle in the collision zone. The latter does not explain the origin of the 8-
314 10 Ma kinematic change. Molnar and Stock (2009) proposed that the growth of the Himalayas
315 increased the gradient of gravitational potential energy, resulting in an increase in stress applied on the
316 Indian plate and its boundaries. However, the Himalaya-Tibet reached its present-day altitude some 15
317 Ma, and probably earlier (Yuan et al., 2013). Late Miocene deformation at India's plate boundaries
318 may have occurred once the stress induced by gravitational potential energy exceeded some threshold
319 value. Onset of widespread deformation in the Indian Ocean may relate to strength loss of the oceanic
320 lithosphere in relation with fault selective abandonment (Delescluse et al., 2008a) and further
321 serpentinization (Delescluse and Chamot-Rooke, 2008b). Delescluse and Chamot-Rooke (2007) and
322 Copley et al. (2010) alternatively proposed that the driving forces resulted from changes in the slab-
323 pull forces at Sunda subduction. Whatever the driver, the 8-9 Ma episode of deformation within Indo-
324 Australian plate modified the kinematics at all surrounding plate's boundaries.
325
326 5. 4. *Implications for the Indian monsoon and environmental changes*
327 The seafloor of the Owen Ridge was significantly uplifted at ~8.5 Ma above the lysocline, inducing
328 the apparent dominance of *G. bulloides* since 8.5 Ma (Shipboard Scientific Party, 1989; Kroon et al.,
329 1991) unrelated to monsoon intensification (Huang et al., 2007). The Late Miocene change in
330 Foraminifera abundances therefore reflects a change in their conditions of preservation rather than a
331 climatic change.
332 In absence of any monsoon intensification at 8.5 Ma, the origin of the coeval environmental change in
333 the Siwalik sequence in Pakistan is enigmatic. This environmental change is characterized by a shift

334 from the dominance of C_3 to C_4 plants in the vegetation (C_3 and C_4 plants using a different
335 photosynthesis pathway) (Quade et al., 1989; Cerling et al., 1997; Molnar, 2005). The estimated
336 decrease in annual precipitation (~120 mm), the increase in annual temperature (+3°C), as well as the
337 decrease in atmospheric CO_2 (Cerling et al., 1997) at ~8-9 Ma cannot account for the ecological
338 transition alone (Nelson, 2006; Huang et al., 2007). Huang et al. (2007) propose that the ecological
339 transition resulted from a large-scale hydrological change over Pakistan and he Himalayan foreland,
340 but the origin of this hydrological change is unknown.
341 Tectonic processes involved in surface uplift act at a different time-scale and are less precisely dated
342 than ecological and climatic changes, making any relationship based on synchronicity difficult to
343 assess. However, the environmental change is coeval with several indicators of surface uplift in
344 Pakistan that might have helped the environmental transition through Indus River avulsion (Fig. 8),
345 which provides a likely origin for the hydrological change pointed out by Huang et al. (2007). Indeed,
346 the Makran underwent a structural reorganization in Late Miocene while the frontal thrust migrated
347 southward. Folds reaching altitudes of 1000-2000 m according to field works (McCall, 1997; Ellouz
348 Zimmerman et al., 2007) triggered a huge submarine olistostrome (~42 000 km^3) (Burg et al., 2008).
349 The Kirthar, Sulaiman and Salt ranges also underwent complex structural reorganizations during the
350 Late Miocene. These structural reorganizations favoured a complex episode of avulsion of the Indus
351 River over more than 400 km (Waheed and Wells, 1990; 1992), which is at its present-day location
352 since only 5 Ma (Clift and Blusztajn, 2005). Surface uplift in Pakistan reduced monsoon precipitation
353 coming from the ocean and increased aridity, without affecting the seasonality (consistently with
354 environment reconstructions of Nelson, 2006). Surface uplift also explains the greater fraction of
355 precipitation coming from continental sources in the Siwalik area, revealed by geochemical studies of
356 Huang et al. (2007). The complex interplay between precipitation source changes (Huang et al., 2007)
357 and Indus avulsion (Waheed and Wells, 1990, 1992) triggered by surface uplift over Pakistan induced
358 successive fragmentations of habitats and the related ecological stresses that lead to the environmental
359 change (Barry et al., 2002).
360
361 **6. Conclusions**

362 The Owen margin, basin and ridge have undergone a significant episode of deformation in the Late
363 Miocene, leading to the uplift of the east Oman margin and the Owen Ridge. The best-dated
364 deformation is the anticline structure on the Oman margin, bracketed between 8.2 and 8.8 Ma. This
365 episode of deformation corresponds to the transition from the Early-Middle Miocene India-Arabia
366 plate boundary to the Owen Fracture Zone. The Late Miocene episode of deformation at the India-
367 Arabia plate boundary is coeval with intraplate deformation in the Central Indian Ocean, suggesting a
368 possible common cause.
369 The uplift of the Owen Ridge induced changes in the condition of preservation of Foraminifera,
370 which confirms the previous assumption of Huang et al. (2007) that the apparent increase in *G.*
371 *Bulloides* at 8.5 Ma is not related to a climatic change. The monsoon might have already been strong
372 at 10 Ma, then decreasing over the Arabian Sea until ~5 Ma (Clift et al., 2008; Prasanta and Sinha,
373 2010; Sakai et al., 2010). Proxies recording changes in summer monsoon intensity east of India, i.e.
374 Chinese loess, abundances of *N. dutertrei* in South China Sea, windblown record in northeast Pacific
375 (Molnar et al., 2010; Steinke et al., 2010), may reflect a shift in the trajectory of atmospheric eddies
376 involved in the Indian monsoon that did not affect the western Indian Ocean. Contouritic drifts lay on
377 the Late Miocene highs (Fig. 7), leading to the hypothesis that the uplift of the Owen Basin edges may
378 also have changed the conditions of record of deep-sea current activity. The arising working
379 hypothesis is that the general increase in carbonate preservation recorded in the Indian Ocean
380 (Peterson et al., 1992) may be the result of the 8-9 Ma-old episode of seafloor uplift rather than the
381 expression of a major climatic or deep-sea circulation change.
382 The questioning of the 8.5 Myrs monsoon intensification suggests that surface uplift in the Pakistan
383 may be responsible for the coeval environmental change recorded in the Siwalik sequence. This
384 environmental change influenced the evolution of mammals in the Late Miocene (Barry et al., 2002;
385 Elton, 2008), including *Sivapithecus,* a likely ancestor of *Pongo pygmae* (Andrews and Cronin, 1982),
386 who disappeared in Pakistan following the ~8.5Ma ecological change (Begun, 2004).
387
388 **Acknowledgements**

We are grateful to Captain Rémi De Monteville, officers and crew members of the BHO Beautemps-Beaupré, and to the GENAVIR team and the hydrographer D. Levieuge for their help in data acquisition. Processing of the Owen-2 dataset was carried out using the Geocluster 5000 software from CGGVeritas.We thank A. Rabaute who helped the organization of the Owen-2 cruise, J. Smith for scientific discussions, and P. Dubernet and N. Bacha for technical assistance. J. Bull, T. Henstock and an anonymous reviewer provided very constructive and careful comments that helped us to improve the manuscript and clarify our thoughts. This study was supported by SHOM, IFREMER, INSU-CNRS, and CEA (LRC Yves-Rocard).

Figure captions

Figure 1 : Bathymetric map of the Arabian Sea, with location of ODP and DSDP drilling sites. The multibeam bathymetric coverage is draped over SRTM-PLUS topography (Becker et al., 2009). Inset shows the regional tectonic setting of the India-Arabia plate boundary, and the position of the summer Inter-Tropical Convergence Zone (ITCZ). AOC : Aden-Owen-Carlsberg triple junction.

Figure 2 : Bathymetric maps of the central (a) and southern (b) portions of the Owen Basin, and location of the seismic lines. See Fig. 1 for location. The bathymetry shows the offset of the Owen Ridge by the Owen Fracture Zone (OFZ). DSDP and ODP Sites are shown by red stars.

Figure 3 : Seismic profiles crossing a) the Oman continental margin, b) the Southern Owen Ridge, c) the Central Owen Ridge (see Fig. 2 for location). Insets show close-views of the seismic profiles in the area of deep-sea drilling (ODP and DSDP) locations. The stratigraphic framework is summarized on the lower left hand corner. Profile a) displays a major anticline structure affecting chalk-rich turbiditic deposits that is overlapped by a 8 Ma-old contouritic drift, composed of pelagic ooze with inserted MTDs. Older events, including an upper-Eocene unconformity, and the obduction of Masirah Ophiolites, are not discussed in this study. Profile b) shows a W-E seismic profile crossing the Southern Owen Ridge at the location of ODP Site 722. The basement, drilled at DSDP Site 224, consists of 50-55 Ma-old basaltic lamprophyres. A major unconformity is observed on the western side of the ridge, where early miocene turbiditic deposits (Unit 4) onlap oligocene deposits drilled at

DSDP site 224. Unit 3 corresponds to a pelagic layer and ends at 10.4 Ma. The overlying Unit 2 is composed of radiolarian rich pelagic chalk and ends at 8.2 Ma. Unit 1 is composed of pelagic ooze and chalk, and dissected by landslide failures. c) shows an W-E seismic profile crossing the Central Owen Ridge. A major unconformity, corresponding to a hiatus of 6 Myr, has been drilled at DSDP Site 223, together with Late Miocene mass transport deposits. The overlying cover is mainly composed of pelagic chalk and ooze, with a detrital component in the Owen Basin. Late Miocene breccias, correlated with an unconformity on the central ridge, have been drilled at DSDP Site 223.

Figure 4 : Seismic profile crossing the Oman margin, showing a major anticline affecting Miocene sediments. See Fig. 2b (top left hand corner) for location, and Fig. 3 for stratigraphic legend.

Figure 5 : a) and b) Seismic profiles crossing the top of the Owen Ridge, highlighting the fanning pattern of early Miocene turbidites. c) Seismic profile crossing the eastern foot of the Southern Owen Ridge, showing a buried system of folds corresponding to the syn-uplift deformation. d) Seismic profile crossing partly buried reliefs in the middle of the Owen Basin. It displays an unconformity draped by 0.3s TWT of pelagic sediments, similar to the Late Miocene unconformity observed on the Central Owen Ridge. See Fig. 2 for profiles location.

Figure 6 : Seismic profiles crossing the Southern Owen Ridge. Profile a) shows a N-S section that displays the Late Miocene fanning marking the uplift of the Owen Ridge. A dense network of faults, with irregular offsets, affects Unit 1 to 4, and may result from fluid escapes. Profile b) shows a transverse section of the southernmost extremity of the southern ridge. It shows that the ridge is formed by folded Indus sediments, crosscut to the east by an fossil vertical fault, interpreted as a fracture zone corresponding to the India-Arabia plate boundary. The present-day Owen Fracture Zone is observed on the western side of the ridge, where it is associated with the Beautemps-Beaupré basin. Profile c) shows a fracture zone at the eastern foot of the southern ridge, and compressive deformation in the overlying sediments. Profile d) shows a series of folds located south of the Beautemps-Beaupré Basin.

445 See Fig. 2 for location and Fig. 3 for stratigraphic legend.

446

447 **Figure 7** : Seismic profiles crossing the eastern side of the Central Owen Ridge. Profile a) shows an
448 angular unconformity sealed by Late Miocene turbidites according to the nearby DSDP Site 222.
449 fracture zone is observed at the eastern foot of the ridge, the present-day active boundary being
450 localized at the mid-slope of the ridge. Profile b) shows the Late Miocene angular unconformity
451 formed during the uplift of the Owen Ridge. See fig.2b for location and fig. 3 for stratigraphic legend.

452

453 **Figure 8 :** Sketches of the geological history of the India-Arabia plate boundary, and the Owen Basin
454 since the Middle Miocene. At ~10 Ma, the India-Arabia plate boundary was located close to the Owen
455 Ridge, which was mostly buried under Indus turbiditic system, excepted a few highs standing above
456 the seafloor. Pakistan was flooded by the Indus delta (Ellouz-Zimmerman et al., 2007). Around 8.5
457 Ma, the Owen Ridge and the Oman margin uplifted, inducing a better preservation of pelagic
458 foraminifera on their top. This event is coeval with general plate reorganization recognized overall the
459 Indian Ocean. The Makran Subduction Zone underwent a major structural reorganization during
460 Tortonian (McCall, 1997), marked by olistostromes (Burg et al., 2008) and a geographic isolation of
461 paleontological species with regards to the area east of the Kirthar Ranges (Ellouz-Zimmerman et al.,
462 2007). The precise location of the frontal thrust in Tortonian is currently unknown. Since 3-6 Ma, the
463 Miocene India-Arabia plate boundary jumped to the Owen Fracture Zone emplaced with large
464 stepover basins along strike. The Oman margin subsided down below the sea level. The Indus river is
465 at its present-day location since ~5-6 Ma (Clift and Blusztajn, 2005).

466

467 **References**

468 An, Z., Kutzbach, J.E., Prell, W.L., Porter, S.C., 2001.Evolution of Asian monsoons and phased uplift
469 of the Himalaya–Tibetan plateau since Late Miocene times. Nature 411, 62–66.

470 Andrews, P., and Cronin, J. E., 1982. The relationships of Sivapithecus and Ramapithecus and the
471 evolution of the orang-utan. Nature 297, 541-546.

472 Bache, F., Leroy, S., Baurion, C., Robinet, J., Gorini, C., Lucazeau, F., Razin, P., d'Acremont, E., Al-

473 Toubi, K., 2010. Post-rift uplift of the Dhofar margin (Gulf of Aden). Terra nova 23, 11-18,
474 DOI: 10.1111/j.1365-3121.2010.00975.x, 2010.
475 Barry, J., Morgan, M. E., Flynn, L. J., Pilbeam, D., Behrensmeyer, A. K., Raza, S. M., Khan, I. A.,
476 Bagdley, C., Hicks, J., Kelley, J., 2002. Faunal and environmental change in the late Miocene
477 Siwaliks of northern Pakistan. Paleobiology 28, 1-71, http://dx.doi.org/10.1666/0094-
478 8373(2002)28[1:FAECIT]2.0.CO;2
479 Brackenridge, R. E., Hernandez-Molina, F. J., Stow, D. A. V., Llave, E, 2013. A Pliocene mixed
480 contourite-turbidite system offshore the Algarve Margin, Gulf of Cadiz: Seismic response, margin
481 evolution and reservoir implications. Mar. Pet. Geol. 46, 36-50,
482 http://dx.doi.org/10.1016/j.marpetgeo.2013.05.015
483 Becker, J. J., Sandwell, D. T., Smith, W. H. F., Braud, J, Blinder, B., Depner, J., Fabre, D., Factor, J.,
484 Ingalls, S., Kim, S-H., Ladner, R., Marks, K., Nelson, S., Pharaoh, A., Trimmer, R., Von
485 Rosenberg, J., Wallace, G., Weatherall, P., 2009. Global bathymetry and elevation data at 30 arc
486 second resolution : SRTM30 PLUS. Marine Geodesy 32, 355-371, doi:
487 10.1080/01490410903297766
488 Begun, D. R., 2004. Sivapithecus is east and Dryopithecus is west, and never the twain shall meet.
489 Anthropological science 113, 53-64.
490 Bernard, A. and Munschy, M., 2000. Le bassin des Mascareignes et le bassin de Laxmi (océan Indien
491 occidental) se sont-ils formés à l'axe d'un même centre d'expansion ? C. R. Acad. Sci. Paris, 330,
492 777–783
493 Bonatti, E., Ligi, M., Gasperini, L., Peyve, A., Raznitsin, Y., Chen, Y. J., 1994. Transform migration
494 and vertical tectonics at the Romanche fracture zone, equatorial Atlantic. J. Geophys. Res. 99,
495 21779-802.
496 Bonatti, E., Brunelli, D., Buck, W. R., Cipriani, A., Fabretti, P., Ferrante, V., Gasperini, L., Ligi, M.,
497 2005. Flexural uplift of a lithospheric slab near the Vema transform (Central Atlantic) : timing and
498 mechanisms. Earth. Planet. Sci. Lett. 240, 642-655.
499 Bourget, J., Zaragosi, S., Rodriguez, M., Fournier, M., Garlan, T., Chamot-Rooke, N., 2013. Late
500 Quaternary megaturbidites of the Indus Fan : origin and stratigraphic significance. Mar. Geol. 336,

10-23, doi:10.1016/j.margeo.2012.11.011.2013

Buck., W. R., 1993. Effect of lithospheric thickness on the formation of high- and low-angle normal faults. Geology 21, 933-936.

Bull, J. M., and Scrutton, R. A., 1990. Fault reactivation in the central Indian Ocean and the rheology of oceanic lithosphere. Nature 344, 855-858.

Bull, J. M., and Scrutton, R. A., 1992. Seismic reflection images of intraplate deformation, central Indian Ocean, and their tectonic significance. J. Geol. Soc. London 149, 955-966.

Bull, J. M., DeMets, C., Krishna, K. S., Sanderson, D. J., Merkouriev, S., 2010. Reconciling plate kinematic and seismic estimates of lithospheric convergence in the central Indian Ocean. Geology 38, 307-310, doi: 10.1130/G30521.1

Burg, J.P., Bernoulli, D., Smit, J., Dolati, A., Bahroudi, A., 2008. A giant catastrophic mud-and-debris flow in the Miocene Makran. Terra Nova 20, 188–193, doi: 10.1111/j.1365-3121.2008.00804.x

Calvès, G., 2008.Tectonostratigraphic and climatic record of the NE Arabian Sea, Ph.D. thesis, 305 pp., Univ. of Aberdeen, Aberdeen U. K.

Cartwright, J. A., 1994. Episodic basin-wide fluid expulsion from geo-pressured shale sequences in the North Sea Basin. Geology 22, 447-450.

Cerling, T.E., Harris, J.M., MacFadden, B.J., Leakey, M.G., Quade, J., Eisenmann, V.,Ehleringer, J.R., 1997.Global vegetation change through the Miocene/Pliocene boundary. Nature 389, 153-158.

Chamot-Rooke, N., Jestin, F., DeVoogd, B., 1993. Intraplate shortening in the central Indian-ocean determined from a 2100-km-long north-south deep seismic-reflection profile. Geology 21(11), 1043–1046.

Cochran, J. R., 1981. The Gulf of Aden: structure and evolution of a young ocean basin and continental margin. J. Geophys. Res. 86, 263-287.

Cochran, J. R., et al., 1989. Intraplate deformation and Bengal fan sedimentation: background and objectives. Proc. Ocean Drill. Program Initial Rep. 116, 3-11.

Clark, M. K., 2012. Continental collision slowing due to viscous mantle lithosphere rather than topography, Nature 483, 74–77, doi:10.1038/nature10848

Clift, P. D., Shimizu, N., Layne, G. D., Blusztain, J. S., Gaedicke, C., Schluter, H.-U., Clark,M. K.,

529 Amjad, S., 2001.Development of the Indus Fan and its significance for the erosional history of the
530 Western Himalaya and Karakoram.Geol. Soc. Am. Bull. 113, 1039–1051.
531 Clift, P. D., Gaedicke, C., 2002. Accelerated mass flux to the Arabian Sea during the middle to late
532 Miocene. Geology 30, 207-210, doi:10.1130/0091-13(2002)030<0207:AMFTTA>2.0.CO;2Clift, P.
533 D., 2006. Controls on the erosion of Cenozoic Asia and the flux of clastic sediment to the ocean.
534 Earth Planet. Sci. Lett. 241, 571-580.
535 Clift, P. D., Hodges, K. V., Heslop, D., Hannigan, R., Van Long, H., Calvès, G., 2008. Correlation of
536 Himalayan exhumation rates and Asian monsoon intensity. Nat. Geosci. 1, 875-880,
537 doi:10.1038/ngeo351
538 Clift, P. D., 2010. Enhanced global continental erosion and exhumation driven by Oligo-Miocene
539 climate change. Geophys. Res. Lett. 37, L09402, doi:10.1029/2010GL043067
540 Cloething, S., Beekman, F., Ziegler, P. A., van Wees, J-D., Sokoutis, D., 2008. Post-rift compressional
541 reactivation potential of passive margins and extensional basins. Geol. Soc. London Spec. Publ.
542 306, 27-70.
543 Copley, A., Avouac, J-P., Royer, J-Y., 2010. India-Asia collision and the Cenozoic slowdown of the
544 Indian plate: implications for the forces driving plate motions. J. Geophys. Res. 115, B03410,
545 doi:10.1029/2009JB006634
546 Delescluse, M., and Chamot-Rooke, N., 2007. Instantaneous deformation and kinematics of the India-
547 Australia Plate. Geophys. J. Int. 168, 818-842, doi: 10.1111/j.1365-246X.2006.03181.x
548 Delescluse, M., Montési, L. G. J., Chamot-Rooke, N., 2008a. Fault reactivation and selective
549 abandonment in the oceanic lithosphere. Geophys. Res. Lett. 35, L16312,
550 doi:10.1029/2008GL035066.
551 Delescluse, M., and Chamot-Rooke, N., 2008b. Serpentinization pulse in the actively deforming
552 Central Indian Basin. Earth Planet. Sci. Lett., v. 276, p. 140-151.
553 DeMets, C., Gordon, R., Royer, J-Y., 2005. Motion between the Indian, Capricorn and Somalian
554 plates since 20 Ma : implications for the timing and magnitude of distributed lithospheric
555 deformation in the equatorial Indian Ocean. Geophys. J. Int. 161, 445-468, doi: 10.1111/j.1365-
556 246X.2005.02598.x

557 DeMets C., Gordon, R. G., Argus, D.F., 2010.Geologically current plate motions. Geophys. J. Int. 181,
558 1-80, doi: 10.1111/j.1365-246X.2009.04491.x.
559 Dupont-Nivet, G., Hoorn, C., Konert, M., 2008. Tibetan uplift prior to the Eocene-Oligocene climate
560 transition : Evidence from pollen analysis of the Xining Basin. Geology 36, 987-990, doi:
561 10.1130/G25063A.1
562 Dyment, J., 1998. Evolution of the Carlsberg Ridge between 60 and 45 Ma: Ridge propagation,
563 spreading asymmetry, and the Deccan-Reunion hotspot. J. Geophys. Res. 103, 24067–24084
564 DOI: 10.1029/98JB01759.
565 Edwards, R.A., Minshull, T. A., White, R. S., 2000. Extension across the Indian–Arabian plate
566 boundary: the Murray Ridge. Geophys. J. Int. 142, 461-477.
567 Edwards, R. A., Minshull, T. A., Flueh, E. R., Kopp, C., 2008. Dalrymple Trough: An active oblique-
568 slip ocean-continent boundary in the northwest Indian Ocean. Earth Planet. Sci. Lett. 272, 437-445.
569 Ellouz Zimmermann, N., Deville, E., Müller, C., Lallemant, S., Subhani, A. B., Tabreez, A. R., 2007.
570 Impact of sedimentation on convergent margin tectonics : example of the Makran Accretionary
571 prism (Pakistan). Thrust Belts and Foreland Basins: From Fold Kinematics to Hydrocarbon
572 Systems, edited by O. L. Lacombe et al., pp. 327–350, Springer, Berlin.
573 Ellouz Zimmermann, N. et al., 2007. Offshore frontal part of the Makranaccretionary prism (Pakistan)
574 the Chamak Survey. Thrust Belts and Foreland Basins: From Fold Kinematics to Hydrocarbon
575 Systems, edited by O. L. Lacombe et al., pp. 349–364, Springer, Berlin.
576 Faugères, J.C., Stow, D.A.V., Imbert, P., Viana, A., 1999.Seismic features diagnostic of contourite
577 drifts. Mar. Geol. 162, 1-38.
578 Fournier, M., Bellahsen, N., Fabbri, O., Gunnell, Y., 2004. Oblique rifting and segmentation of the NE
579 Gulf of Aden passive margin. Geochem. Geophys. Geosyst. 5, Q11005,
580 doi:10.1029/2004GC000731
581 Fournier, M., Chamot-Rooke N., Petit C., Fabbri O., Huchon P., Maillot B., Lepvrier C., 2008a. In-
582 situ evidence for dextral active motion at the Arabia-India plate boundary. Nat. Geosci. 1, 54-58,
583 doi:10.1038/ngeo.2007.24.
584 Fournier, M., Petit C., Chamot-Rooke N., Fabbri O., Huchon P., Maillot B., Lepvrier, C., 2008b) Do

585 ridge-ridge-fault triple junctions exist on Earth? Evidence from the Aden-Owen-Carlsberg junction
586 in the NW Indian Ocean. Basin Research 20, 575-590.doi: 10.1111/j.1365-2117.2008.00356.x
587 Fournier, M., Chamot-Rooke, N., Petit, C., Huchon, P., Al-Kathiri, A., Audin, L., Beslier, M.-O.,
588 d'Acremont, E., Fabbri, O., Fleury, J.-M., Khanbari, K., Lepvrier, C., Leroy, S., Maillot B.,
589 Merkouriev, S., 2010.Arabia-Somalia plate kinematics, evolution of the Aden-Owen-Carlsberg
590 triple junction, and opening of the Gulf of Aden. J. Geophys. Res. 115, B04102,
591 doi:10.1029/2008JB006257
592 Fournier, M., Chamot-Rooke N., Rodriguez, M., Huchon, P., Petit, C., Beslier, M.-O., Zaragosi S.,
593 2011. Owen Fracture Zone: the Arabia-India plate boundary unveiled. Earth Planet. Sci. Lett. 302,
594 247-252, doi:10.1016/j.epsl.2010.12.027.
595 Gaedicke, C., Prexl, A., Schlüter, H.U., Roeser, H., Clift, P., 2002. Seismic stratigraphy and
596 correlation of major regional unconformities in the northern Arabia Sea.The Tectonic and Climatic
597 Evolution of the Arabian Sea Region, edited by Clift, P. D., Kroon, D., Gaedicke, C., & Craig, J.,
598 Geol. Soc. Spec. Publ. 195, 25-36.
599 Gunnell, Y., Carter, A. Petit, C., Fournier, M., 2007. Post-rift seaward downwarping at passive
600 margins: new insights from southern Oman using stratigraphy to constrain apatite fission-track and
601 (U-Th)/He dating, Geology 35, 647-650, doi:10.1130/G23639A.1
602 Harris, N. B. W., 2006, The elevation of the Tibetan Plateau and its impact on the monsoon.
603 Palaeogeography Palaeoclimatology Palaeoecology 241, 4-15.
604 Harrison, T.M., Copeland, P., Kidd, W.S.F., Yin, A., 1992. Raising Tibet. Science 255, 1663-1670.
605 Henstock, T. J.,Minshull, T. A., 2004. Localized rifting at Chagos bank in the India-Capricorn plate
606 boundary zone. Geology 32, 237–240.
607 Hiscott, R. N., Pickering, K. T.,Bouma, A. H., Hand, B. M., Kneller, B. C.,Postma, G.,Soh, W.,1997.
608 Basin-Floor Fans in the North Sea: Sequence Stratigraphic Models vs. Sedimentary Facies:
609 Discussion. AAPG bull. 81, 662-665
610 Huang, Y., Clemens, S. C., Liu, W., Wang, L., Prell, W. L., 2007. Large-scale hydrological change
611 drove the Late Miocene C4 plant expansion in the Himalayan foreland and Arabian Peninsula.
612 Geology 35, 531-534.

613 Kolla, V., Bé, A. W. H., Biscaye, P. E., 1976. Calcium Carbonate distribution in the surface sediments
614 of the Indian Ocean. J. Geophys. Res. 81, 2605-2616.
615 Krishna, K. S., Bull, J. M., Scrutton, R. A., 2009. Early (pre-8 Ma) fault activity and temporal strain
616 accumulation in the central Indian Ocean. Geology 37, 227-230, doi: 10.1130/G25265A.1
617 Kroon, D., Steens, T.,Troelstra, S.R., 1991. Onset of monsoonal related upwelling in the western
618 Arabian Sea as revealed by planktonic foraminifers. In Prell, W.L., Niitsuma, N., et al.,
619 Proceedings of the Ocean Drilling Project, Sci. Results, 117, 257- 263 College Station, Texas
620 (Ocean Drilling Program).
621 Lepvrier, C., Fournier, M. Bérard, T. Roger, J., 2002. Cenozoic extension in coastal Dhofar (southern
622 Oman): Implications on the oblique rifting of the gulf of Aden. Tectonophysics 357, 279-293.
623 Leroy, S. et al., 2010. From rifting to oceanic spreading in the Gulf of Aden: a synthesis.
624 Arab.J.Geosci. doi 10.1007/s12517-011-0475-4
625 Marches E., Mulder T., Gonthier E., Hanquiez V., Cremer M., Garlan T., Lecroart P., 2010. Perched
626 lobes formation induced by contourite construction in the Gulf of Cadiz: Interactions between
627 gravity processes and contour currents (Algarve Margin, South Portugal), Sedimentary Geology
628 229, 81-94.
629 McCall, G.J.H., 1997. The geotectonic history of the Makran and adjacent areas of southern Iran. J.
630 Asian Earth Sci., 15, 517-531.
631 Mercuriev, S., DeMets, C., 2006.Constraints on Indian plate motion since 20 Ma from dense Russian
632 magnetic data: Implications for Indian plate dynamics. Geochem. Geophys.Geosyst. 7, Q02002,
633 doi:10.1029/2005GC001079.
634 Molnar, P., England, P., 1990. Late Cenozoic uplift of mountain ranges and global climatic change:
635 chicken or egg? Nature 346, 29-34.
636 Molnar, P., England, P., Martinod, J., 1993. Mantle dynamics, uplift of the Tibetan Plateau, and the
637 Indian monsoon. Rev. Geophys. 31, 357–396.
638 Molnar, P., 2005. Mio-Pliocene Growth of the Tibetan Plateau and Evolution of East Asian Climate.
639 Palaeontologia Electronica 8, 1-23.

640 Molnar, P., Stock, J., 2009. Slowing of India's convergence with Eurasia since 20 Ma and its
641 implications for Tibetan mantle dynamics. Tectonics, 28, TC3001, doi:10.1029/2008TC002271
642 Molnar, P., Boos, W. R., Battisti, D. S., 2010. Orographic controls on climate and paleoclimate of
643 Asia: thermal and mechanical role of the Tibetan Plateau. Annu. Rev. Earth Planet. Sci. 38, 77-102.
644 Mountain, G. S.,Prell, W.L., 1990.A multiphase plate tectonic history of the southeast continental
645 margin of Oman. The Geology and Tectonics of the Oman Region, edited by Robertson, A. H. F.,
646 Searle, M. P. and Ries, A. C., Geol. Soc. Spec. Publ., 49, 725-743.
647 Nelson, S., 2006. Isotopic reconstructions of habitat change surrounding the extinction of
648 Sivapithecus, a Miocene hominoid, in the Siwalik Group of Pakistan. Paleaogeo., Paleaoclim.,
649 Palaeoeco. 243, 204-222.
650 Peterson, L. C., Murray, D. W., Ehrmann, W. U., Hempel, P., 1992.Cenozoic carbonate accumulation
651 and compensation depth changes in the Indian Ocean. In Synthesis of results from scientific
652 drilling in the Indian Ocean, ed. RA Duncan, DK., Rea, R. B. Kidd, U. von Rad, J. K., Weissel,
653 Geophys. Monogr. 70, 311-333. Am. Geophys. Union, Washington, D. C.
654 Petit, C., Fournier, M., Gunnell, Y., 2007.Tectonic and climatic controls on rift escarpments: Erosion
655 and flexural rebound of the Dhofar passive margin (Gulf ofAden, Oman), J. Geophys. Res. 112,
656 B03406, doi:10.1029/2006JB004554
657 Piper, D. J. W., Normark, W. R., 1983.Turbidite depositional patterns and flow characteristics, Navy
658 Submarine Fan, California Borderland. Sedimentology 30, 681-694.DOI: 10.1111/j.1365-
659 3091.1983.tb00702.x
660 Platel, J.P., Roger, J., 1989. Evolution géodynamique du Dhofar (Sultanat d'Oman) pendant le Crétacé
661 et le Tertiaire en relation avec l'ouverture du golfe d'Aden, Bull. Soc. Géol. France 2, 253-263.
662 Prasanta, S., Sinha, R., 2010.Evolution of the Indian summer monsoon: synthesis of continental
663 records. From: Clift, P. D., Tada, R. & Zheng, H. (eds) Monsoon Evolution and Tectonics–Climate
664 Linkage in Asia. Geological Soc. London, Spec. Publ., 342, 153–183.
665 Quade, J., Cerling, T.E., Bowman, J.R., 1989. Development of Asian monsoon revealed by marked
666 ecological shift during the latest Miocene in northern Pakistan. Nature 342, 163-166.

667 Qayyum, M., Lawrence, R. D., Niem, A. R., 1997. Discovery of the palaeo-Indus delta-fan complex.
668 Journal of the Geological Society 154, 753-756, doi:10.1144/gsjgs.154.5.0753
669 Rodriguez, M., Fournier, M., Chamot-Rooke, N., Huchon, P., Bourget, J., Sorbier, M., Zaragosi, S.,
670 Rabaute, A., 2011.Neotectonics of the Owen Fracture Zone (NW Indian Ocean): structural
671 evolution of an oceanic strike-slip plate boundary. Geochem., Geophys., Geosyst. 12,
672 doi:10.1029/2011GC003731.
673 Rodriguez, M., Fournier, M., Chamot-Rooke, N., Huchon, P., Zaragosi, S., Rabaute, A., 2012. Mass
674 wasting processes along the Owen Ridge (NW Indian Ocean). Mar. Geol. 326-328, 80-100, doi:
675 10.1016/j.margeo.2012.08.008
676 Rodriguez, M., Chamot-Rooke, N., Hébert, H., Fournier, M., Huchon, P. 2013. Owen Ridge deep-
677 water submarine landslides: Implications for tsunami hazard along the Oman coast, NHESS, 13,
678 417–424.
679 Rodriguez, M., Chamot-Rooke, N., Fournier, M., Huchon, P., Delescluse, M. 2013. Mode of opening
680 of an oceanic pull-apart: The 20 °N Basin along the Owen Fracture Zone (NW Indian Ocean),
681 Tectonics 32, 1-15, doi:10.1002/tect.20083.
682 Rowley, D. B., Currie, B. S., 2006. Palaeo-altimetry of the late Eocene to Miocene Lunpola basin,
683 central Tibet. Nature 439, 677-681.
684 Royer, J. Y., Chaubey, A. K., Dyment, J., Bhattacharya, G. C., Srinivas, K., Yateesh, V.,
685 Ramprasad,T., 2002.Paelogene plate tectonic evolution of the Arabian and Eastern Somali basins.in
686 The Tectonic and Climatic Evolution of the Arabian Sea Region, edited by P. D. Clift et al., Geol.
687 Soc. Spec. Publ., 195, 7–23Shipboard Scientific Party 1989, Site 731, Proc. Ocean. Drill. Program
688 Initial Rep., 117, 585–652.
689 Shipboard Scientific Party, 1974, Site 222, In R.B. Whitmarsh, O.E. Weser, and D.A. Ross, DSDP
690 Init. Repts, 23, doi:10.2973/dsdp.proc.23.106.
691 Sakai, T., Saneyoshi, M., Sawada, Y., Nakatsukasa, M., Mbua, E., Ishida, H., 2010. Climate shift
692 recorded at around 10 Ma in Miocene succession of Samburu Hills, northern Kenya Rift, and its
693 significance. From: Clift, P. D., Tada, R. &Zheng, H. (eds) Monsoon Evolution and Tectonics–
694 Climate Linkage in Asia. Geol. Soc., London, Spec. Publ. 342,109-127, doi:10.1144/SP342.9

695 Smit, J., Burg, J-P., Dolati, a., Sokoutis, D., 2010. Effects of mass waste events on thrust wedges:
696 Analogue experiments and application to the Makran accretionary wedge. Tectonics 29, TC3003,
697 doi:10.1029/2009TC002526.
698 Spicer, R. A., Harris, N. B. W., Widdowson, M., Herman, A. B., Guo, S., Valdes, P.J., Wolfe, J. A.,
699 and Kelley, S. P., 2003, Constant elevation of southern Tibet over the past 15 million years. Nature
700 421, 622-624.
701 Steinke, S., Groeneveld, J., Johnstone, H., and Rendle-Bühring, R., 2010. East Asian summer
702 monsoon weakening after 7.5 Ma: Evidence from combined planktonic foraminifera Mg/Ca and
703 δ18O (ODP Site 1146; northern South China Sea). Palaeogeography, Palaeoclimatology,
704 Palaeoecology 289, 33-43.
705 Sun, X., and Wang, P., 2005. How old is the Asian monsoon system? Palaeobotanical records from
706 China. Palaeogeography, Palaeoclimatology, Palaeoecology 222, 181-222.
707 Waheed, A., Wells, N. A., 1990. Changes in paleocurrents during the development of an obliquely
708 convergent plate boundary (Sulaiman fold-belt, southwestern Himalayas, west-central Pakistan).
709 Sedimentary Geology 67, 237-261.
710 Waheed, A., Wells, N. A., 1992. Fluvial history of late Cenozoic molasse, Sulaiman range, Pakistan.
711 Geol. Bull. Univ. Peshawar 25, 1-15.
712 Wang, P., Steven Clemens, S., Beaufort, L., Braconnot, P., Ganssene, G., Jiana, Z., Kershawf, P.,
713 Sarntheing, M., 2005. Evolution and variability of the Asian monsoon system: state of the art and
714 outstanding issues. Quaternary Sci. Rev. 24, 595–629.
715 Wang, E., Kirby, E., Furlong, K. P., van Soest, M., Xu, G., Shi, X., Kamp, P. J. J., Hodges, K. V.,
716 2012. Two-phase growth of high topography in eastern Tibet during Cenozoic. Nat. Geosci. 5,
717 640–645, doi:10.1038/ngeo1538
718 Weissel, J. K., Anderson, R. N., Geller, C. A., 1980. Deformation of the Indo-Australian plate. Nature
719 287, 284-291.
720 Weissel, J.K., Childers, V.A., Karner, G.D., 1992. Extensional and Compressional Deformationof the
721 Lithosphere in the Light of ODP Drilling in the Indian Ocean.Synthesisof Results from Scientific
722 Drilling in the Indian Ocean. : Geophysical Monograph70, American Geophysical Union.

723 Whitmarsh, R.B., 1979. The Owen Basin off the south-east margin of Arabia and the evolution of the
724 Owen Fracture Zone. Geophysical Journal of the Royal Astronomical Society 58, 441-470.
725 Wiens, D. A., Demets, C., Gordon, R. G., Stein, S., Argus, D., Engeln, J. F., Lundgren, P., Quible, D.,
726 Stein, C.,Weinstein, S., Woods,D. F., 1985. A diffuse plate boundary model for Indian ocean
727 tectonics. Geophys. Res.Lett. 12, 429–432.
728 Yuan, D-Y., et al., 2013. The growth of northeastern Tibet and its relevance to large-scale continental
729 geodynamics: a review of recent studies. Tectonics 32, 1-13, doi:10.1002/tect.20081
730

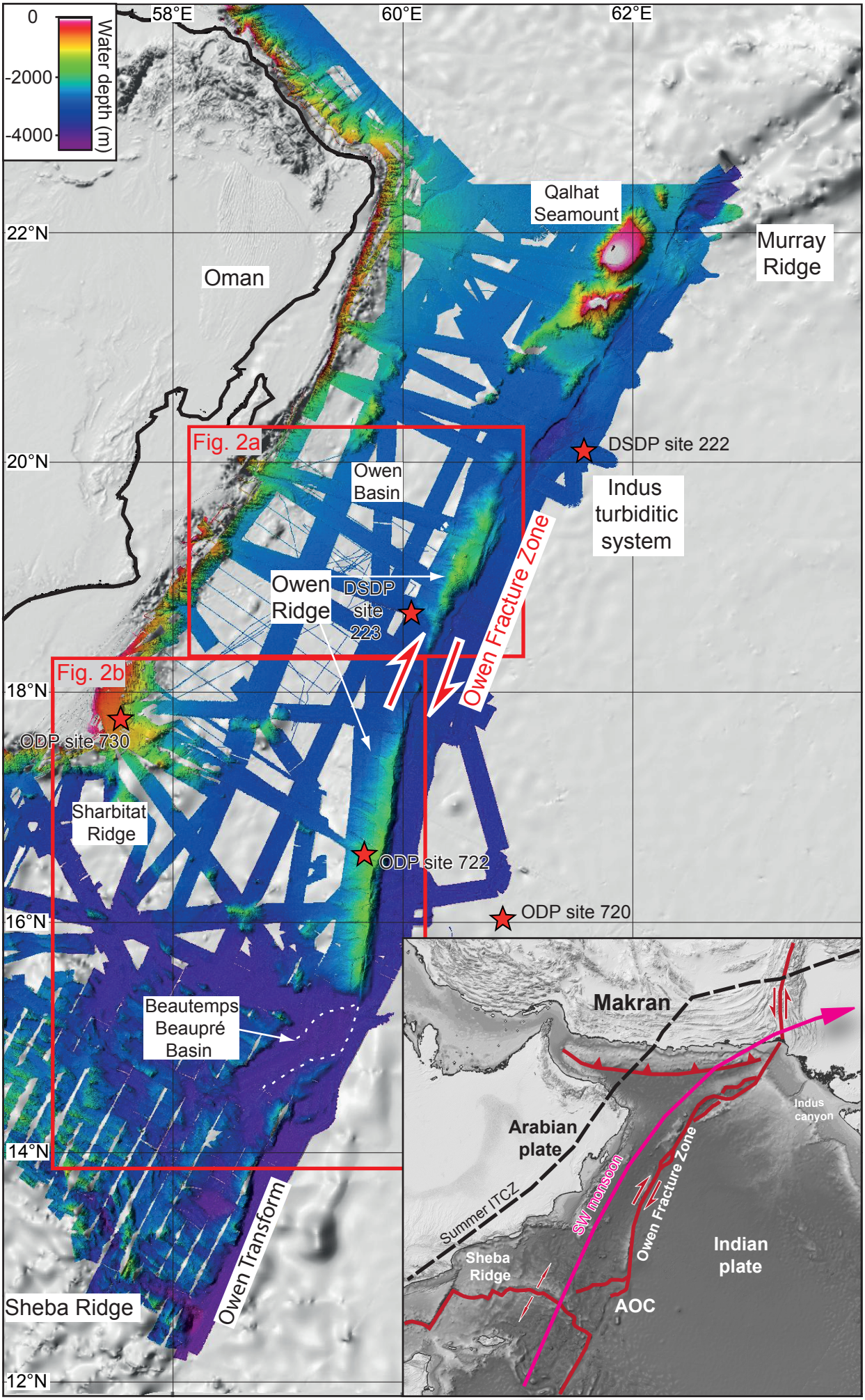
0
-2000
-4000
Water depth (m)
58°E
60°E
62°E
22°N
20°N
18°N
16°N
14°N
12°N
Oman
Qalhat Seamount
Murray Ridge
Fig. 2a
Fig. 2b
DSDP site 222
Indus turbiditic system
Owen Basin
Owen Ridge
DSDP site 223
Owen Fracture Zone
ODP site 730
Sharbitat Ridge
ODP site 722
ODP site 720
Beautemps Beaupré Basin
Owen Transform
Sheba Ridge
Makran
Arabian plate
Indus canyon
Summer ITCZ
SW monsoon
Owen Fracture Zone
Sheba Ridge
Indian plate
AOC

Figure 1

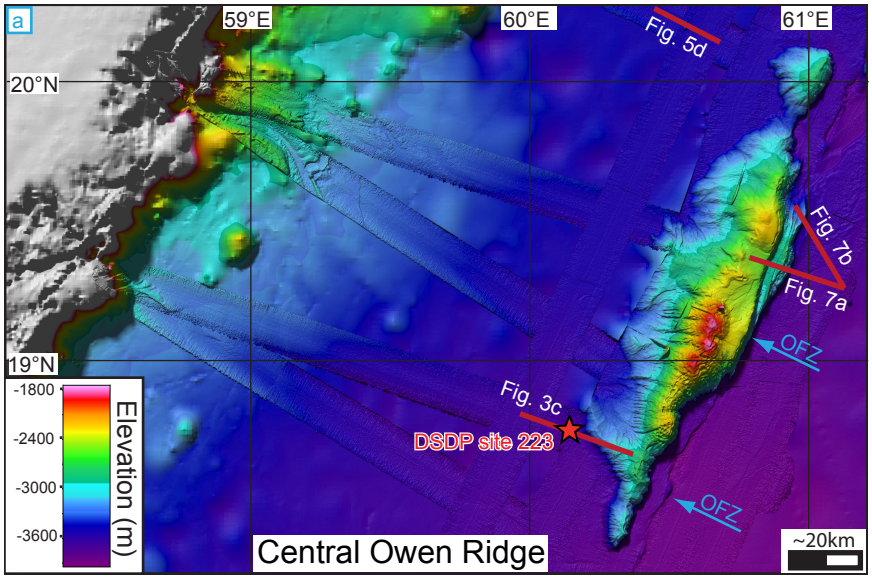
a
59°E
60°E
61°E
20°N
19°N
Fig. 5d
Fig. 7b
Fig. 7a
OFZ
Fig. 3c
DSDP site 223
OFZ
-1800
-2400
-3000
-3600
Elevation (m)
Central Owen Ridge
~20km

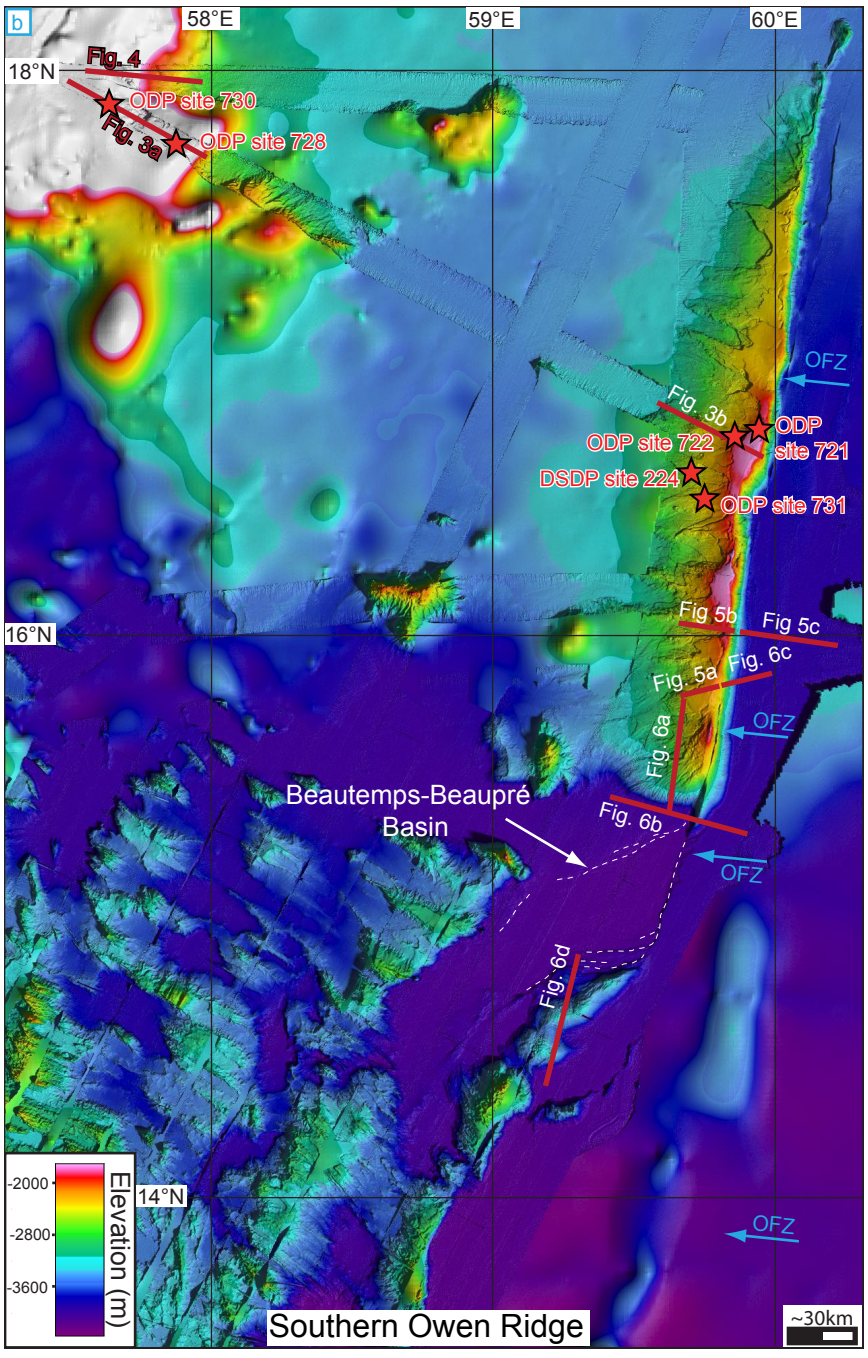
b
58°E
59°E
60°E
18°N
Fig. 4
ODP site 730
Fig. 3a
ODP site 728
OFZ
Fig. 3b
ODP site 722
ODP site 721
DSDP site 224
ODP site 731
16°N
Fig 5b
Fig 5c
Fig. 5a
Fig. 6c
Fig. 6a
OFZ
Beautemps-Beaupré Basin
Fig. 6b
OFZ
Fig. 6d
-2000
-2800
-3600
Elevation (m)
14°N
OFZ
Southern Owen Ridge
~30km

Figure 2

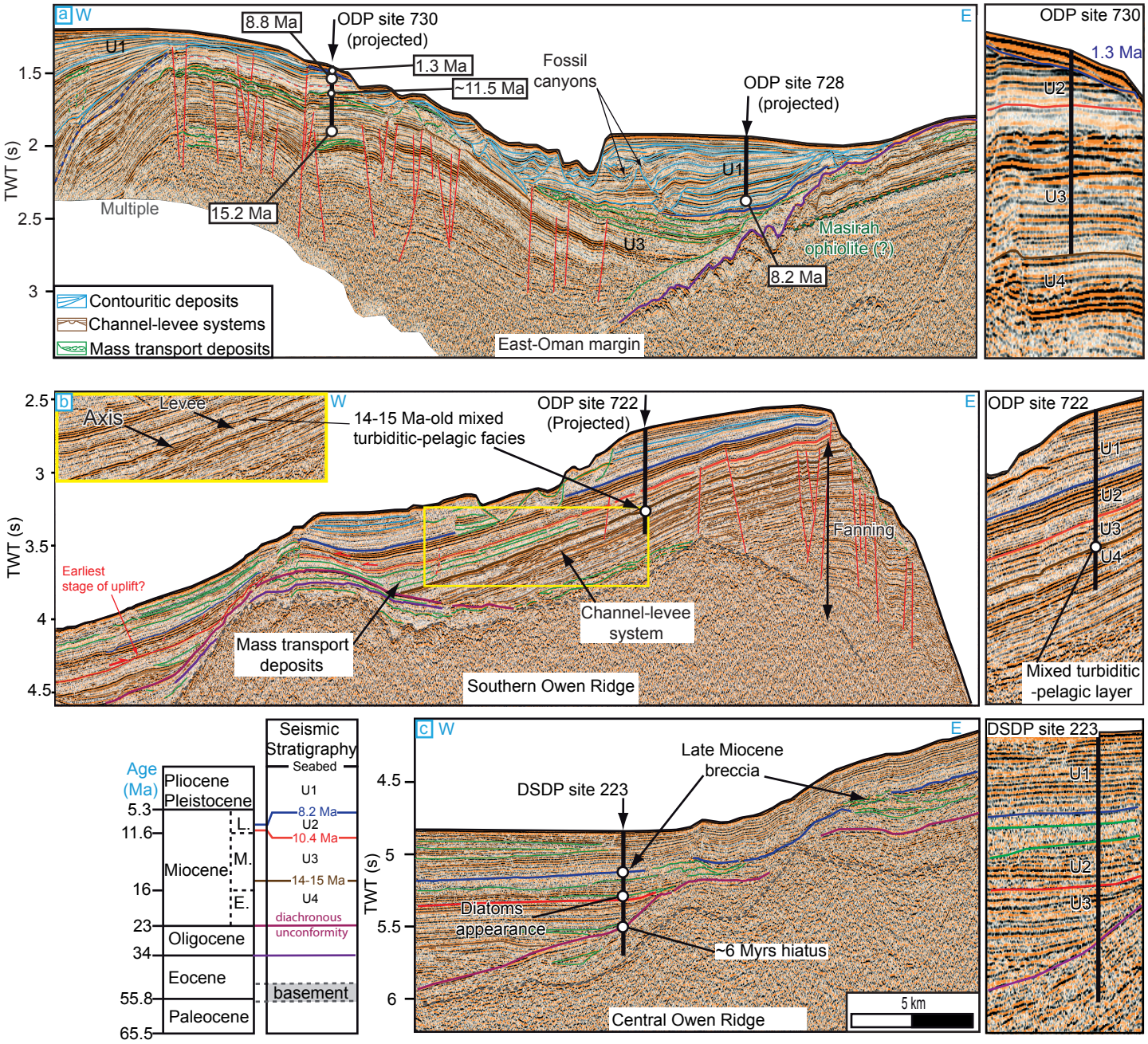
a W
E
8.8 Ma
ODP site 730
(projected)
1.3 Ma
~11.5 Ma
Fossil
canyons
ODP site 728
(projected)
U1
15.2 Ma
Multiple
U3
Masirah
ophiolite (?)
8.2 Ma
East-Oman margin
TWT (s)
1.5
2
2.5
3
Contouritic deposits
Channel-levee systems
Mass transport deposits
ODP site 730
1.3 Ma
U2
U3
U4
b
W
E
Axis
Levee
14-15 Ma-old mixed
turbiditic-pelagic facies
ODP site 722
(Projected)
Fanning
Earliest
stage of uplift?
Channel-levee
system
Mass transport
deposits
Southern Owen Ridge
ODP site 722
U1
U2
U3
U4
Mixed turbiditic
-pelagic layer
2.5
3
3.5
4
4.5
Age
(Ma)
Pliocene
Pleistocene
5.3
11.6
Miocene
L.
M.
E.
16
23
Oligocene
34
Eocene
55.8
Paleocene
65.5
Seismic
Stratigraphy
Seabed
U1
8.2 Ma
U2
10.4 Ma
U3
14-15 Ma
U4
diachronous
unconformity
basement
c W
E
Late Miocene
breccia
DSDP site 223
Diatoms
appearance
~6 Myrs hiatus
Central Owen Ridge
5 km
TWT (s)
4.5
5
5.5
6
DSDP site 223
U1
U2
U3

Figure 3

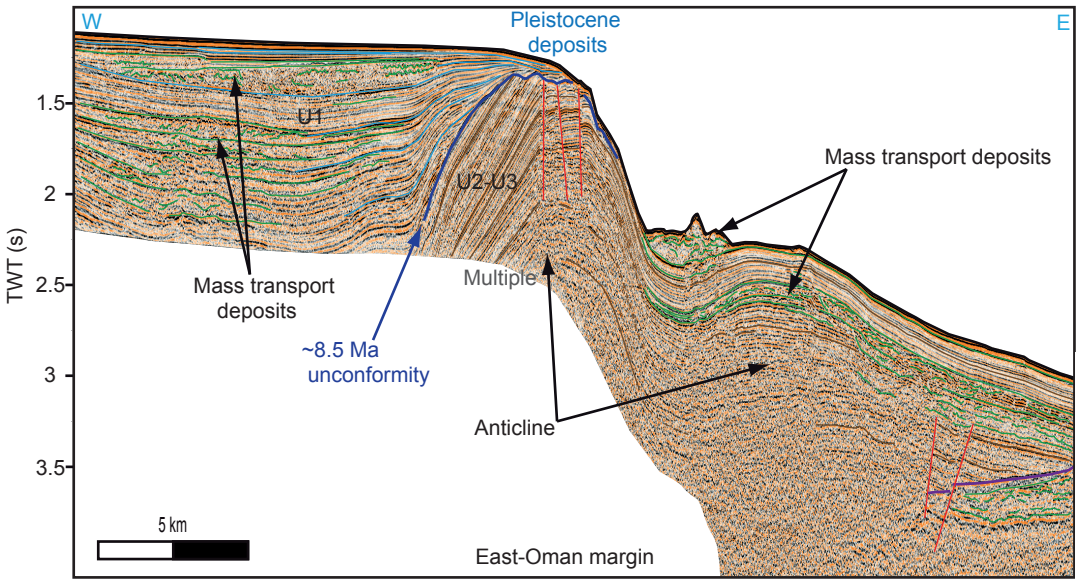
W
Pleistocene
deposits
E
1.5
2
2.5
3
3.5
TWT (s)
U1
U2-U3
Mass transport deposits
Mass transport
deposits
Multiple
~8.5 Ma
unconformity
Anticline
5 km
East-Oman margin

Figure 4

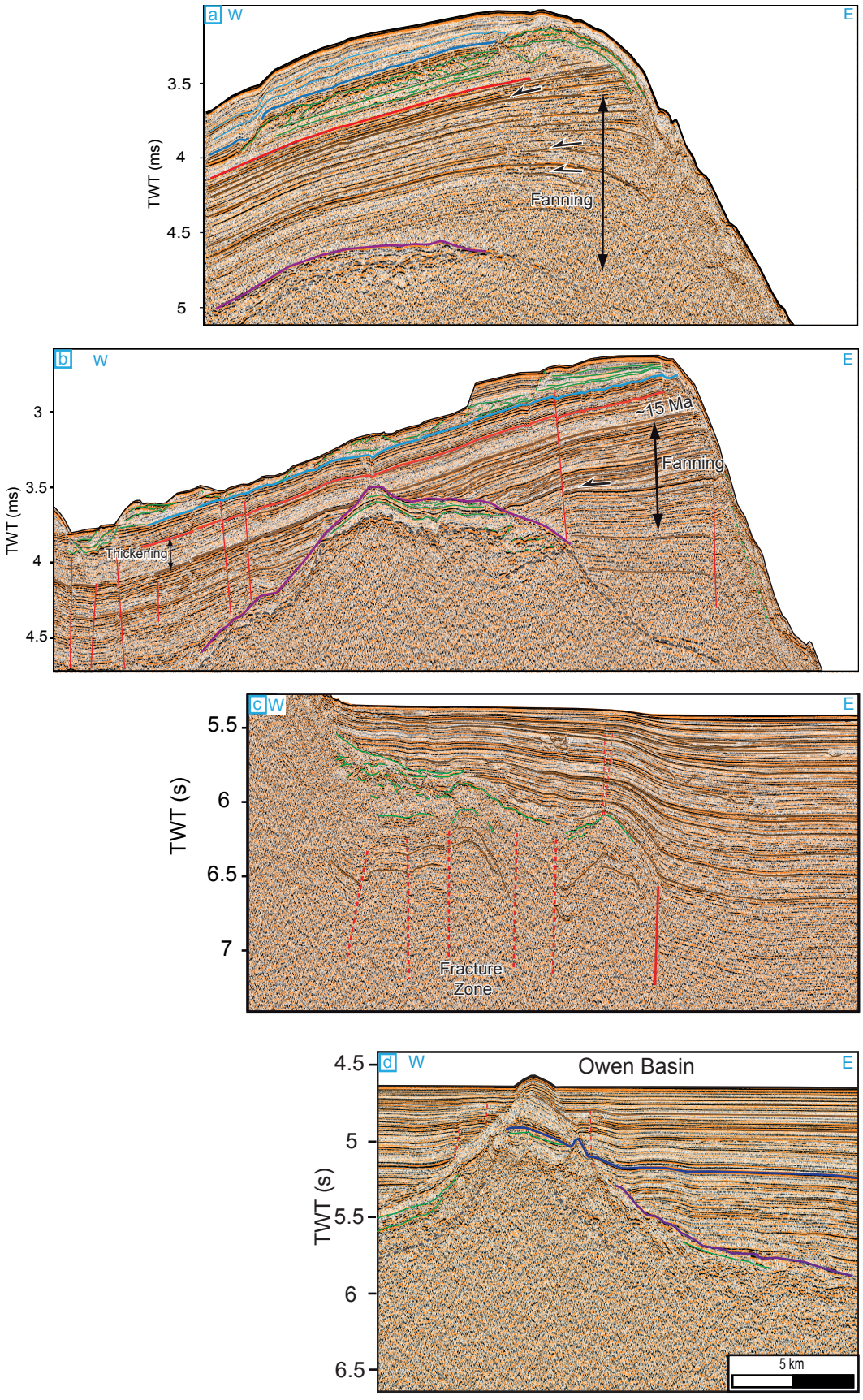
a
W
E
TWT (ms)
3.5
4
4.5
5
Fanning
b
W
E
TWT (ms)
3
3.5
4
4.5
~15 Ma
Fanning
Thickening
c
W
E
TWT (s)
5.5
6
6.5
7
Fracture
Zone
d
W
Owen Basin
E
TWT (s)
4.5
5
5.5
6
6.5
5 km

Figure 5

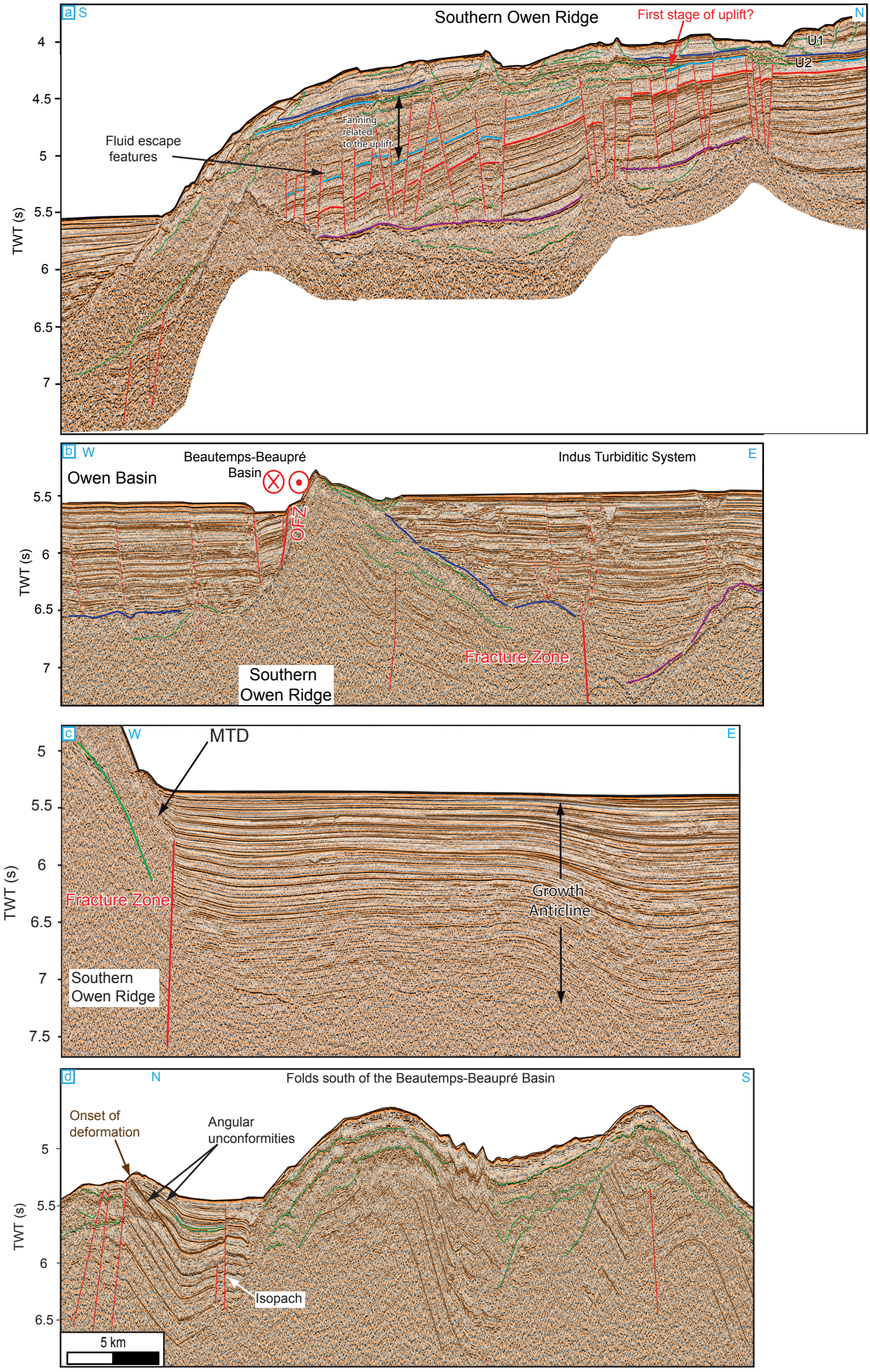
a S
Southern Owen Ridge
First stage of uplift?
N
U1
U2
Fanning related to the uplift
Fluid escape features
TWT (s)
4
4.5
5
5.5
6
6.5
7
b W
Beautemps-Beaupré Basin
Indus Turbiditic System
E
Owen Basin
OFZ
Fracture Zone
Southern Owen Ridge
c W
MTD
E
Fracture Zone
Growth Anticline
Southern Owen Ridge
5
5.5
6
6.5
7
7.5
d N
Folds south of the Beautemps-Beaupré Basin
S
Onset of deformation
Angular unconformities
Isopach
5 km

Figure 6

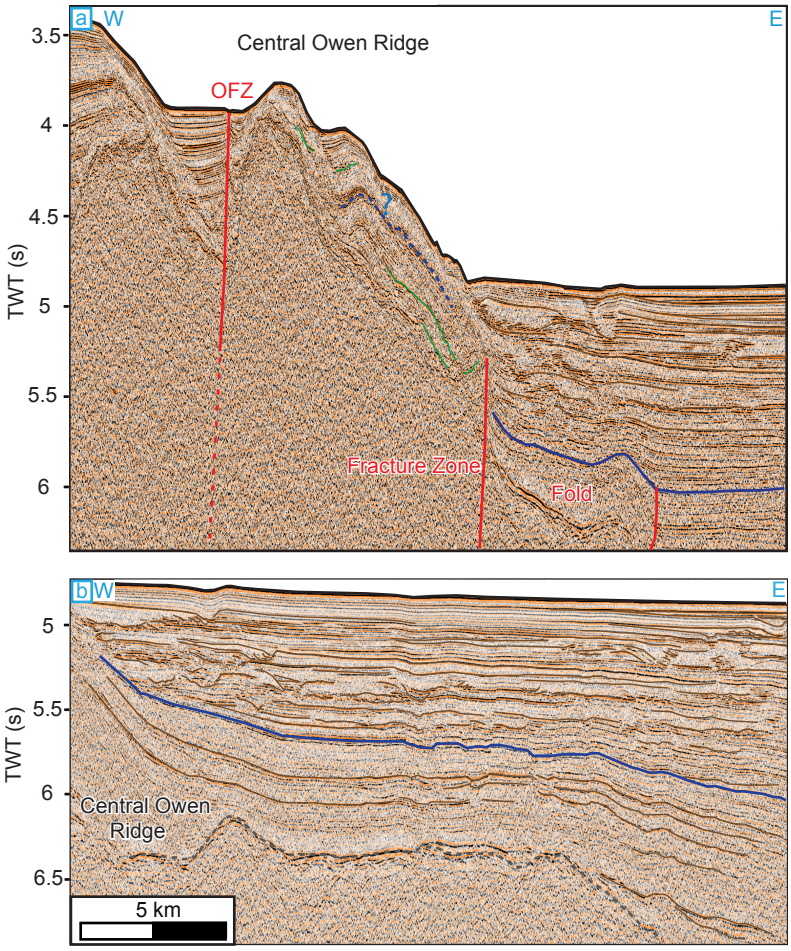
a
W
E
Central Owen Ridge
OFZ
Fracture Zone
Fold
TWT (s)
3.5
4
4.5
5
5.5
6
b
W
E
TWT (s)
5
5.5
6
6.5
Central Owen Ridge
5 km

Figure 7

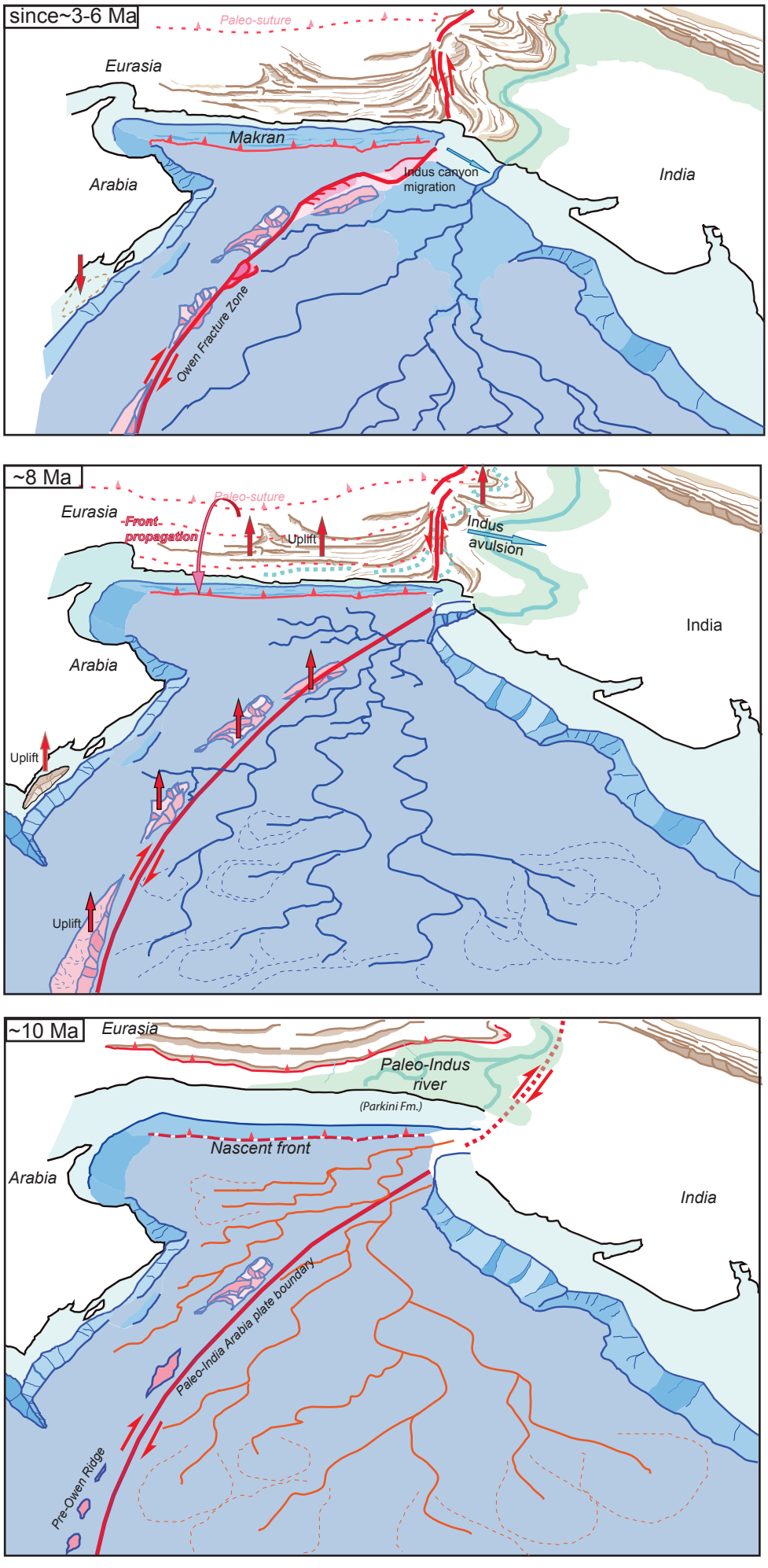
since~3-6 Ma
Paleo-suture
Eurasia
Makran
Arabia
Indus canyon migration
India
Owen Fracture Zone
~8 Ma
Paleo-suture
Eurasia
Front propagation
Uplift
Indus avulsion
India
Arabia
Uplift
Uplift
~10 Ma
Eurasia
Paleo-Indus river
(Parkini Fm.)
Nascent front
Arabia
India
Paleo-India Arabia plate boundary
Pre-Owen Ridge

Figure 8